

## Supporting Information

# Porous and High-strength Graphitic Carbon/SiC Three-Dimensional Electrode for Capacitive Deionization and Fuel Cell Applications

*Yifei Xue,<sup>a</sup> Jiangzhou Xie,<sup>a</sup> Meng He,<sup>a</sup> Mingquan Liu,<sup>a</sup> Min Xu,<sup>a</sup> Wei Ni,<sup>a</sup> and Yi-Ming Yan<sup>\*b</sup>*

<sup>a</sup> School of Chemistry and Chemical engineering, Beijing Institute of Technology, Beijing, 100081, China

<sup>b</sup> State Key Lab of Organic-Inorganic Composites, Beijing Advanced Innovation Center for Soft Matter Science and Engineering, Beijing University of Chemical Technology, Beijing, 100029, China

\*Corresponding author

Email: [bityanyiming@163.com](mailto:bityanyiming@163.com)

## Supporting data

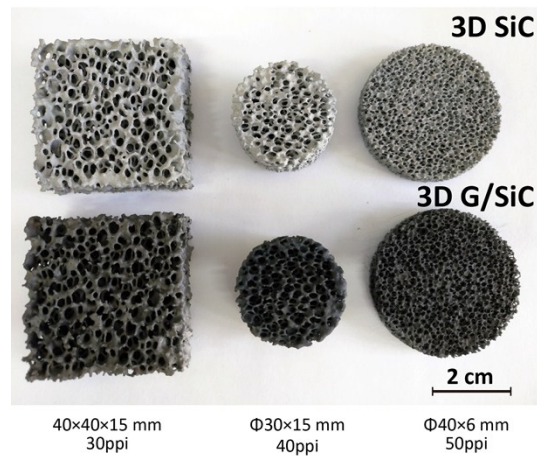


**Figure S1.** Photograph of 3D SiC templates and 3D C/SiC composites in different shape, size and pore density.

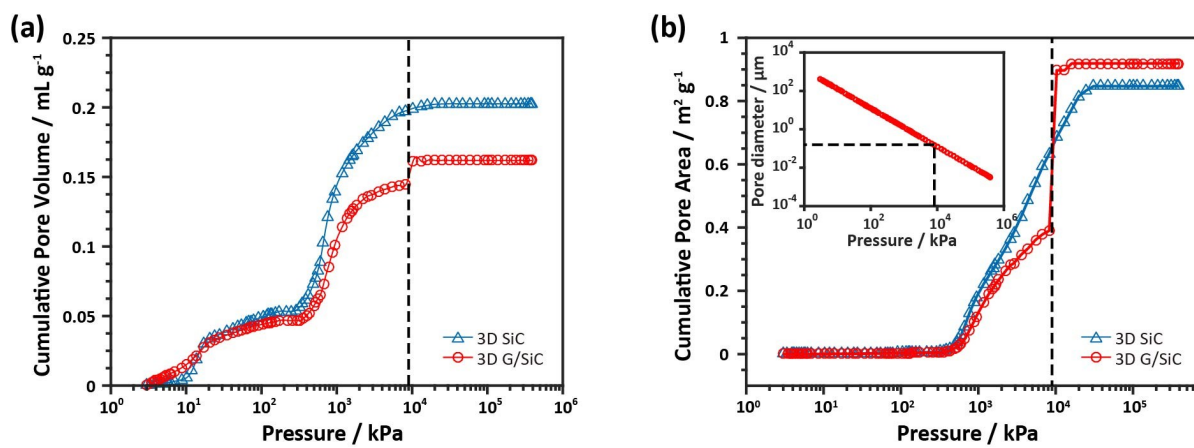


**Figure S2.** a) Cumulative pore volume versus pressure curve of 3D SiC template and 3D G/SiC. b) Cumulative pore area versus pressure curve of 3D SiC template and 3D G/SiC. The inset shows the correlation curve of pore diameter and pressure.

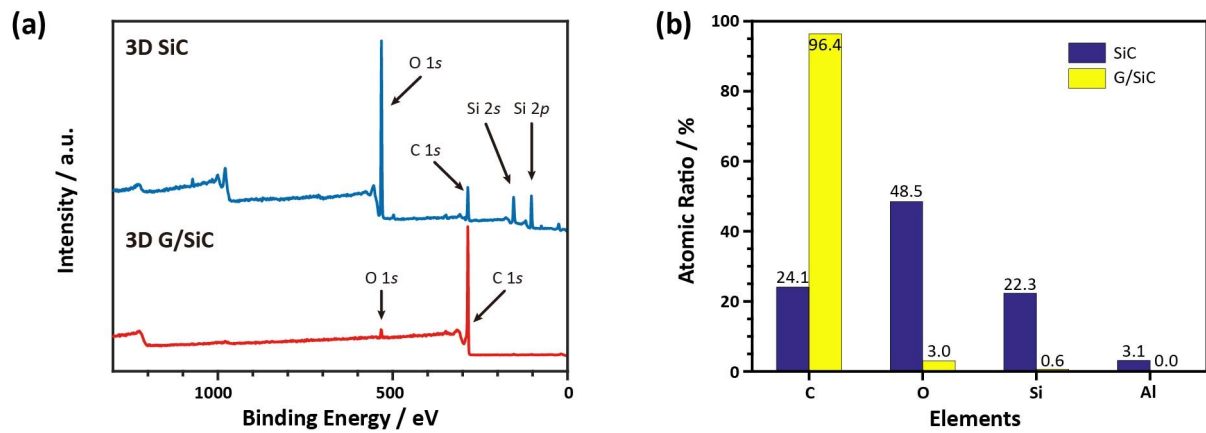


**Figure S3.** a) XPS survey of the 3D SiC template and 3D G/SiC. b) Atomic ratio of 3D SiC template and 3D G/SiC.

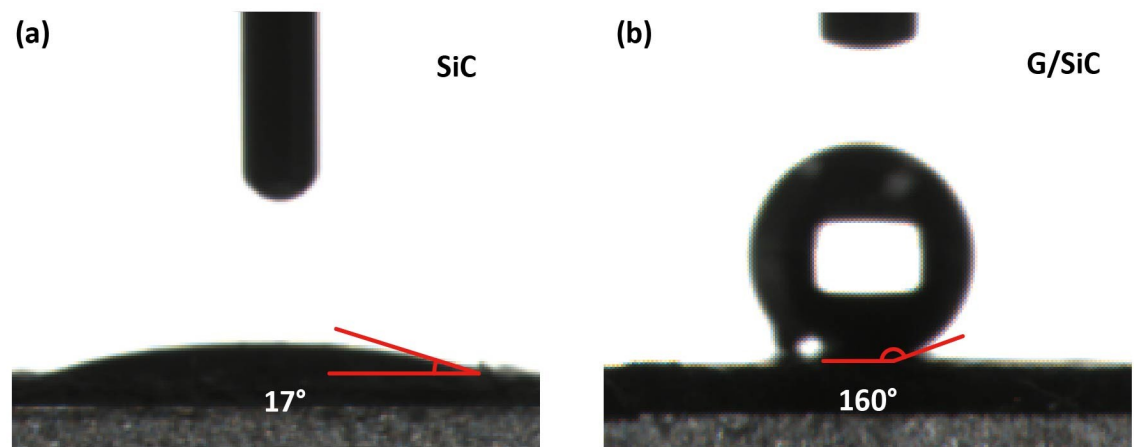


**Figure S4.** Contact angle measurements of a) SiC template and b) G/SiC composite.

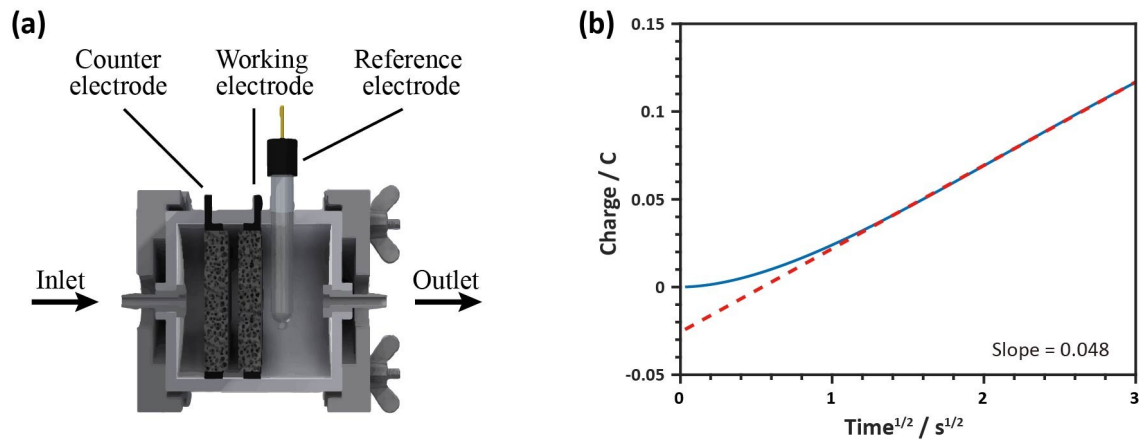


**Figure S5.** a) The internal construction of a specially designed three-electrode cell. b) Charge versus square of time curve for the 3D C/SiC electrode.

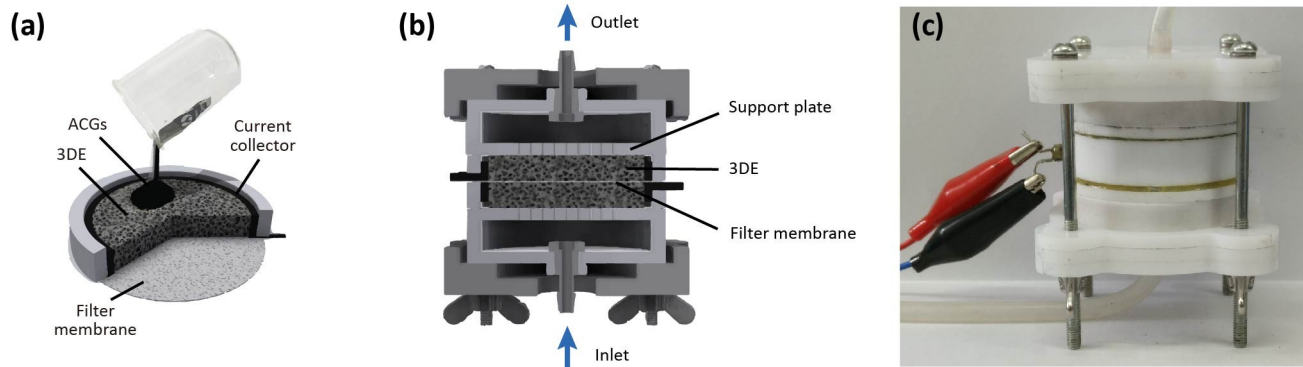


**Figure S6.** a) Schematic representation of the procedure for preparing flow-through electrode by filling ACGs. b) The internal construction of designed flow-through capacitive deionization cell. c) Digital photograph of specially designed CDI cell with one CDI unit.

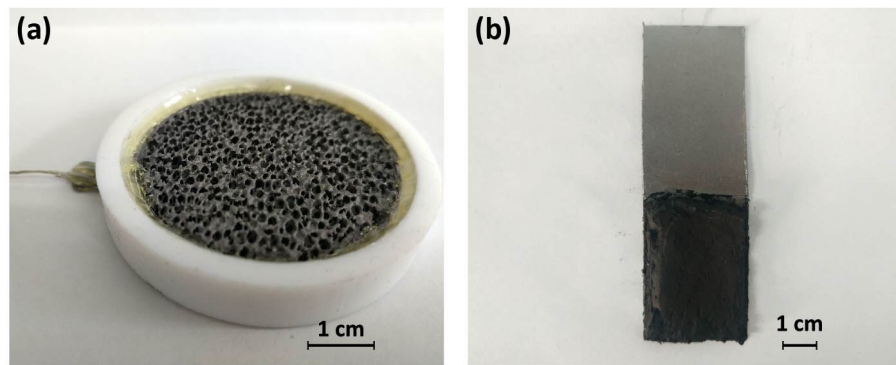


**Figure S7.** Digital photograph of a) 3D G/SiC based flow-through CDI electrode and b) traditional activated carbon electrode.

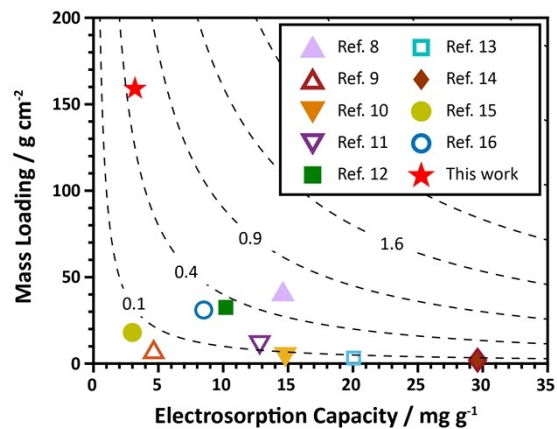


**Figure S8.** Mass loading per unit area vs desalination amount per unit mass plots of 3D G/SiC based CDI cell and recently reported CDI cells. The dashed line indicates the isoline of desalination amount per unit area and the numbers represent the corresponding value in terms of  $\text{mg cm}^{-2}$ .

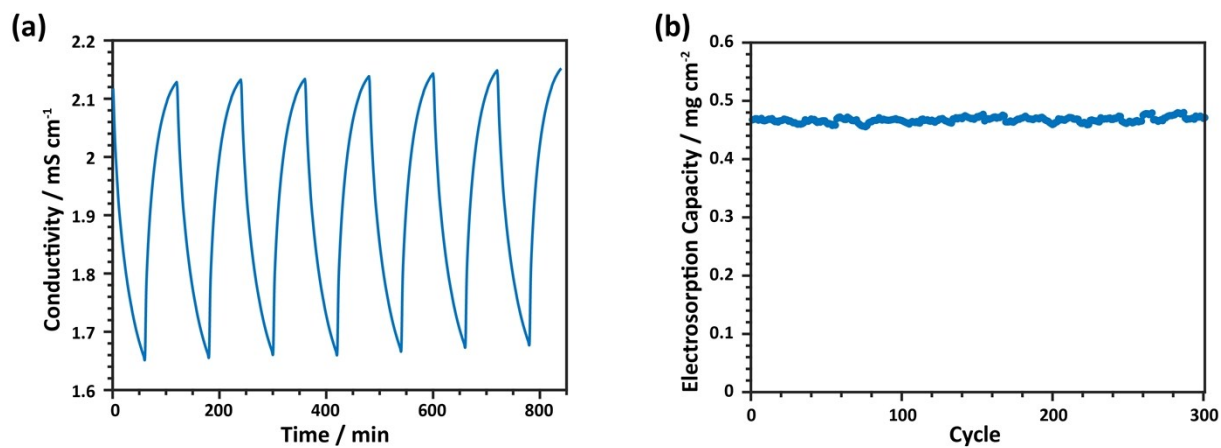


**Figure S9.** a) Adsorption/desorption profiles and b) cycle stability of 3D G/SiC based CDI electrode in the long-term test.

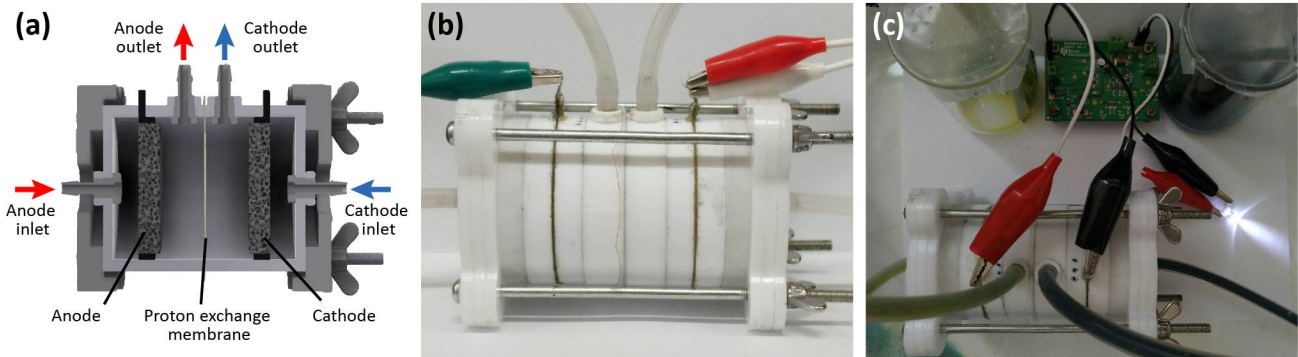


**Figure S10.** a) The internal construction of designed direct biomass fuel cell. b, c) Digital photograph of designed DBFC and lighting up a LED by using DBFC.

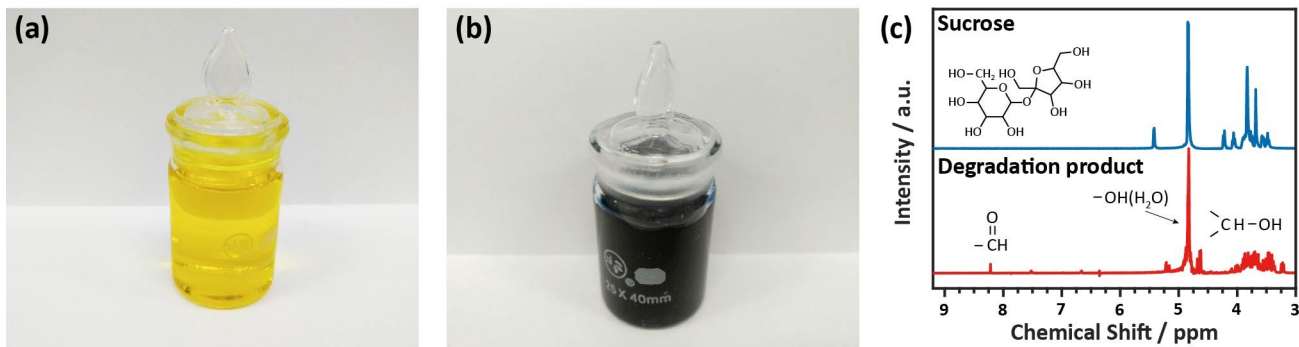


**Figure S11.** a, b) Digital photograph of oxidation state phosphomolybdic acid solution and biomass reduced phosphomolybdic acid solution. c) <sup>1</sup>H NMR spectrum of sucrose solution (blue line) and the final products in the degradation of sucrose (red line).

**Table S1.** Mechanical properties of our 3D SiC, 3D G/SiC and other carbon-based 3D materials.

Materials	Preparation methods	Binder	Compressive strength (MPa)	Young's modulus (MPa)	Regenerable	Ref.
rGO 3D structures	3D printing	Rhodamine modified BCS	0.01	0.13	No	1
Graphene aerogels & SiC	3D printing	Resorcinol formaldehyde resin	-	14	No	2
3D-GN	CVD	None	> 0.9	1.5	No	3
3D-GR	CVD	None	0.15	9.5	No	4
3D SiC	-	None	1.24	40.9	-	This work
3D G/SiC	CVD	None	2.75	43.4	Yes	This work

**Table S2.** Comparison between various CDI cells with different types and electrode materials.

Types <sup>a</sup>	Electrode materials	Binder	Mass loading <sup>b</sup>	Electrode Size (cm)	Voltage (V)	Initial concentration (mg L <sup>-1</sup> )	Electrosorption capacity <sup>c</sup>	Ref.
FB	TiO <sub>2</sub> /CNTs	PTFE	~65 mg	-	1.2	500	4.3 mg g <sup>-1</sup>	5
FB	3D graphene	PTFE	~47 mg	-	1.5	50	4.95 mg g <sup>-1</sup>	6
FB	OMC/CNT	PTFE	1200 mg	-	1.2	40	0.69 mg g <sup>-1</sup>	7
FB	ACE	Hybrid binder	1920 mg 40 mg cm <sup>-2</sup>	4.8x5	1.5	1000	14.6 mg g <sup>-1</sup> 0.58 mg cm <sup>-2</sup>	8
FB	Activated carbon fiber webs	None	~460 mg ~6.5 mg cm <sup>-2</sup>	5x7x0.02	1.6	90	4.64 mg g <sup>-1</sup> ~0.03 mg cm <sup>-2</sup> 1.52 mg cm <sup>-3</sup>	9
FB	NG-CNFs	None	~720 mg ~5.6 mg cm <sup>-2</sup>	8x8	1.2	1000	14.79 mg g <sup>-1</sup> 0.083 mg cm <sup>-2</sup>	10
FB	bc-CNFs	None	800 mg 12.5 mg cm <sup>-2</sup>	8x8 x0.025	1.2	1000	12.81 mg g <sup>-1</sup> 0.080 mg cm <sup>-2</sup> 3.20 mg cm <sup>-3</sup>	11
FB	ZnO-activated carbon cloth	-	520 mg 31.0 mg cm <sup>-2</sup>	2.9x2.9	1.2	100	8.5 mg g <sup>-1</sup> 0.26 mg cm <sup>-2</sup>	12
FB	NHPC	-	320 mg 3.2 mg cm <sup>-2</sup>	6.8x7.3 x0.01	1.4	~520	20.05 mg g <sup>-1</sup> 0.065 mg cm <sup>-2</sup> 6.46 mg cm <sup>-3</sup>	13
FB	HGF	PTFE	110 mg 2.0 mg cm <sup>-2</sup>	6x4.5 x0.26	2.0	572	29.6 mg g <sup>-1</sup> 0.06 mg cm <sup>-2</sup> 0.23 mg cm <sup>-3</sup>	14
FT	Commercial porous ACE	-	110 mg 18.0 mg cm <sup>-2</sup>	1.75x1.75 x0.03	1.0	300	3 mg g <sup>-1</sup> 0.054 mg cm <sup>-2</sup> 1.79 mg cm <sup>-3</sup>	15
FT	Aerogels	None	260 mg 32.5 mg cm <sup>-2</sup>	2x2x0.1	1.5	6000	10.2 mg g <sup>-1</sup> 0.33 mg cm <sup>-2</sup> 3.32 mg cm <sup>-3</sup>	16
FT	3D G/SiC & AC granule	None	4000 mg 159 mg cm <sup>-2</sup>	Φ4x0.6	1.5	1000	3.20 mg g <sup>-1</sup> 0.5 mg cm <sup>-2</sup> 0.85 mg cm <sup>-3</sup>	This work

**Note:** <sup>a)</sup> The codes "FB", "FT" in "Types" represent flow-between and flow-through. <sup>b)</sup> The data in terms of "mg", "mg cm<sup>-2</sup>" in "Mass Loading" refer to the mass of active material in whole cell and unit area of electrode. <sup>c)</sup> The data in terms of "mg g<sup>-1</sup>", "mg cm<sup>-2</sup>" and "mg cm<sup>-3</sup>" in "Electrosorption capacity" refer to the salt adsorption capacity values calculated by per unit mass of active material, per unit area and per unit volume of electrode.

**Table S3.** Comparison between various biomass-powered fuel cells.

Electrode materials	Anode catalyst	Cathode catalyst	Biomass	Biomass concentration (g L <sup>-1</sup> )	Open circuit voltage (V)	Maximum power density (mW cm <sup>-2</sup> )	Ref.
Carbon nanotube fibers	GOx	BOD	Glucose	2.7	0.8	0.74	17
Graphene nanosheets	GOx	BOD	Glucose	18	0.58	0.02	18
Carbon fiber sheet	GDH	BOD	Glucose	72	0.8	1.45	19
3D G/Co <sub>3</sub> O <sub>4</sub>	Co <sub>3</sub> O <sub>4</sub>	Co <sub>3</sub> O <sub>4</sub>	Glucose	36	1.1	2.38	20
Carbon cloth	PMo <sub>12</sub>	Pt/C	Starch	15	0.4	0.44	21
Graphite felt	PW <sub>11</sub> Mo	P <sub>3</sub> Mo <sub>18</sub> V <sub>7</sub>	Starch	40	0.6	1.57	22
Carbon cloth	PMo <sub>12</sub>	PMo <sub>12</sub>	Lignin	25	0.43	0.49	23
3D G/SiC	PMo <sub>12</sub>	PMo <sub>12</sub>	Sucrose	15	0.28	0.12	This work

## Supplementary Movie

### Movie S1. Compression test process of 3D G/SiC

This movie shows the process and real time data of testing the mechanical property of 3D G/SiC.

The movie at:

- 0 s A 3D G/SiC framework is placed on a table mounted material testing system and the compression test is beginning.
- 6 s The compression platen touches the top surface of the 3D G/SiC.
- 119 s Compression stress reaches the yield point of the 3D G/SiC.
- 159 s The compression test is finished.

### Movie S2. Working process of 3D G/SiC based DBFC

This movie shows the working process of 3D G/SiC based DBFC.

The movie at:

- 0-2 s A LED is powered by 3D G/SiC based DBFC.
- 2-5 s Break the circuit and the light turns off.
- 5-14 s Connect the circuit and the LED lights up simultaneously.

## Supporting reference

1. E. Garcia-Tunon, S. Barg, J. Franco, R. Bell, S. Eslava, E. D'Elia, R. C. Maher, F. Guitian and E. Saiz, *Adv. Mater.*, 2015, **27**, 1688-1693.
2. C. Zhu, T. Y. J. Han, E. B. Duoss, A. M. Golobic, J. D. Kuntz, C. M. Spadaccini and M. A. Worsley, *Nat. Commun.*, 2015, **6**, 6962.
3. H. Huang, H. Bi, M. Zhou, F. Xu, T. Lin, F. Liu, L. Zhang, H. Zhang and F. Huang, *J. Mater. Chem. A*, 2014, **2**, 18215-18218.
4. H. Bi, T. Q. Lin, F. Xu, Y. F. Tang, Z. Q. Liu and F. Q. Huang, *Nano Lett.*, 2016, **16**, 349-354.
5. H. B. Li, Y. L. Ma and R. Niu, *Sep. Purif. Technol.*, 2016, **171**, 93-100.
6. Z. Y. Yang, L. J. Jin, G. Q. Lu, Q. Q. Xiao, Y. X. Zhang, L. Jing, X. X. Zhang, Y. M. Yan and K. N. Sun, *Adv. Funct. Mater.*, 2014, **24**, 3917-3925.
7. Z. Peng, D. S. Zhang, T. T. Yan, J. P. Zhang and L. Y. Shi, *Appl. Surf. Sci.*, 2013, **282**, 965-973.
8. J. Z. Xie, Y. F. Xue, M. He, W. C. Luo, H. N. Wang, R. Wang and Y. M. Yan, *Carbon*, 2017, **123**, 574-582.
9. G. Wang, C. Pan, L. P. Wang, Q. Dong, C. Yu, Z. B. Zhao and J. S. Qiu, *Electrochim. Acta*, 2012, **69**, 65-70.
10. Y. Liu, X. T. Xu, T. Lu, Z. Sun, D. H. C. Chua and L. K. Pan, *RSC Adv.*, 2015, **5**, 34117-34124.
11. Y. Liu, T. Lu, Z. Sun, D. H. C. Chua and L. K. Pan, *J. Mater. Chem. A*, 2015, **3**, 8693-8700.
12. M. T. Z. Myint, S. H. Al-Harthi and J. Dutta, *Desalination*, 2014, **344**, 236-242.
13. Z. Wang, T. T. Yan, L. Y. Shi and D. S. Zhang, *ACS Appl. Mater. Interfaces*, 2017, **9**, 15068-15078.
14. J. Li, B. X. Ji, R. Jiang, P. P. Zhang, N. Chen, G. F. Zhang and L. T. Qu, *Carbon*, 2018, **129**, 95-103.
15. E. N. Guyes, A. Simanovski and M. E. Suss, *RSC Adv.*, 2017, **7**, 21308-21313.
16. M. E. Suss, T. F. Baumann, W. L. Bourcier, C. M. Spadaccini, K. A. Rose, J. G. Santiago and M. Stadermann, *Energy Environ. Sci.*, 2012, **5**, 9511-9519.
17. F. Gao, L. Viry, M. Maugey, P. Poulin and N. Mano, *Nat. Commun.*, 2010, **1**, 2.
18. C. Liu, S. Alwarappan, Z. F. Chen, X. X. Kong and C. Z. Li, *Biosens. Bioelectron.*, 2010, **25**, 1829-1833.
19. H. Sakai, T. Nakagawa, Y. Tokita, T. Hatazawa, T. Ikeda, S. Tsujimura and K. Kano, *Energy Environ. Sci.*, 2009, **2**, 133-138.
20. Y. Chen, K. P. Prasad, X. W. Wang, H. C. Pang, R. Y. Yan, A. Than, M. B. Chan-Park and P. Chen, *Phys. Chem. Chem. Phys.*, 2013, **15**, 9170-9176.
21. W. Liu, W. Mu, M. J. Liu, X. D. Zhang, H. L. Cai and Y. L. Deng, *Nat. Commun.*, 2014, **5**, 1-8.
22. F. Xu, H. Li, Y. L. Liu and Q. Jing, *Sci Rep.*, 2017, **7**, 5142.
23. X. B. Zhao and J. Y. Zhu, *ChemSusChem*, 2016, **9**, 197-207.